

The Possible Nature of Dips in the Light Curves of Semi-Detached Binaries with Stationary Disks

D. V. Bisikalo¹, P. V. Kaygorodov¹, A. A. Boyarchuk¹, and O. A. Kuznetsov^{1,2}

¹ *Institute of Astronomy, Pyatnitskaya str. 48, Moscow, 119017 Russia*

² *Keldysh Institute of Applied Mathematics, Russian Academy of Sciences, Miusskaya sq. 4, Moscow, 125047 Russia*

**Published in Astronomy Reports, Vol. 49, N. 9, 2005, pp. 701-708. Translated from
Astronomicheskii Zhurnal, Vol. 82, N. 9, 2005, pp. 788-796**

Abstract

A thickening at the outer edge of the accretion disk is usually invoked to explain the dips in the light curves of cataclysmic variables with stationary disks at phases ~ 0.7 . The non-collisional interaction between the stream and the disk in the stationary solution raises the question of why matter appears at a considerable height above the accretion disk in such systems. Our three-dimensional numerical modeling demonstrates that a thickening of the halo above the disk can appear even in the absence of a direct collision between the stream and the disk. In the gas-dynamical flow pattern described with the "hot-line" model, a considerable fraction of the matter is accelerated in the vertical direction during the flow's interaction with the circumdisk halo. The vertical motion of the gas due to the presence of the z component of the velocity leads to a gradual thickening of the circumdisk halo. The computations reveal the strongest thickening of the halo above the outer edge of the disk at phases ~ 0.7 , in agreement with observations for stationary-disk cataclysmic variables. This supports the hot-line model suggested earlier as a description of the pattern of the matter flows in semi-detached binaries, and presents new possibilities for interpreting the light curves of such systems.

1 Introduction

Observations of low-mass X-ray binaries (LMXBs) have revealed dips in the X-ray light curves for several systems. Explanations of these dips have hypothesized the presence of a thickening at the accretion disk's outer edge at phase ~ 0.8 , which corresponds to the position of this feature in the light curves ([1, 2] and references therein). The presence of matter surrounding the X-ray source at a considerable height above the system's orbital plane, along with the matter's uneven distribution in azimuth, can be explained in terms of either the companion's gravitational action on the accretion disk or the interaction between the stream of matter from the inner Lagrangian point (L_1) and the disk. The coincidence of the phase of the observed dips with the assumed position where the stream from L_1 approaches the outer edge of the disk has tended to focus study on this particular region. Beginning with [3–5], numerical studies of variations of the disk's scale height due to its interaction with the stream were initiated. Currently, the idea that the stream ricochets off the disk's outer edge is considered the best way to explain the presence of matter at heights considerably exceeding the disk thickness. The possibility that the stream flows around the edge of the disk was first discussed in [6–9]; in 1996, the gas-dynamical computations of Armitage and Livio [10] showed

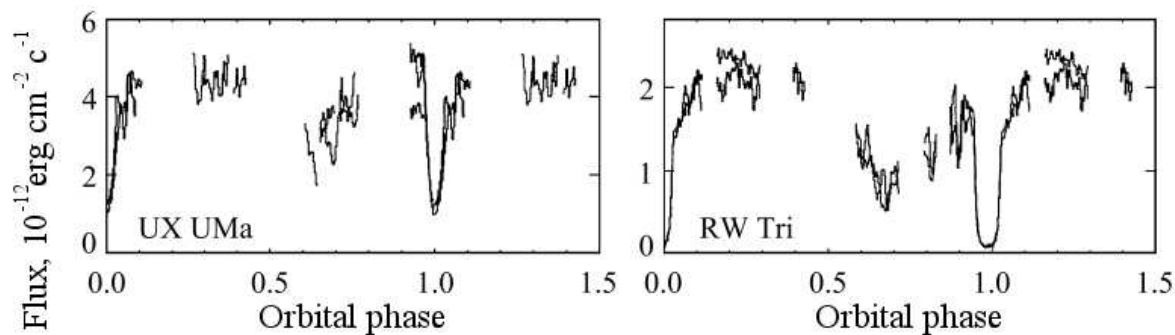


Figure 1: Light curves of the UX UMa (left) and RW Tri (right) systems in the ultraviolet ($1415 \div 1433\text{\AA}$), according to [16].

that a considerable fraction of the stream’s matter can ricochet off the edge of the accretion disk. In their model, after colliding with the disk edge, some of the matter in the stream rises to a considerable height (compared to the disk thickness), forming a stream towards the inner parts of the disk. The computations of [10] demonstrated that this stream of matter could explain the presence of the dips observed in LMXB light curves.

It is easiest to identify dips due to the presence of matter located high above the disk in LMXBs, since they contain a very compact source at the center of the disk. However, similar light-curve features in various wavelength ranges have also been recorded for a number of cataclysmic binaries in outburst, such as U Gem [11, 12], OY Car [13, 14], and Z Cha [15]. Further observations showed that lightcurve dips can also appear when a system is in a stationary state. Studies of the ultraviolet light curves of the eclipsing nova-like cataclysmic binaries UX UMa and RW Tri [16] confirmed this result, and suggested that this phenomenon was universal in semi-detached binaries with accretion disks. As an example, Fig. 1 presents the observed light curves for UX UMa (left panel) and RW Tri (right panel) from [16]. It is interesting that, in contrast to the cataclysmic systems, systems with stationary disks display pre-eclipse dips at much earlier phases¹, $0.6 \div 0.7$ [16, 17] (Fig. 1).

This raises the question of what leads to the presence of matter at considerable heights above the accretion disk in the case of a stationary interaction between the stream and the disk. Gasdynamical studies of the terminal flow pattern in semi-detached binaries demonstrate that the interaction between the stream and the disk is collisionless in this case [18–24]. In contrast to the hot-spot model, which assumes that the stream impacts the edge of the accretion disk, the stream interacts with gas of the circumdisk halo in the stationary case, forming an extended region of enhanced energy release, or so called “hot line”. This means that there will be no ricochet of the stream in the steady-state mode, and hence this model cannot explain the dips in the light curves of binaries with stationary disks.

Our aim here is to study possible ways of thickening the halo above a disk, which give rise to eclipses of the central source and the presence of dips in the light curves during the stationary flow of matter in semidetached binaries. Our three-dimensional modeling of the flow structure demonstrates that, during the stream’s interaction with the circumdisk halo, a considerable fraction of the matter is accelerated in the vertical direction and rises to heights appreciably exceeding the disk scale height. The strongest thickening of the halo above the outer edge of the disk occurs at phase ~ 0.7 , in agreement with observations of systems with a stationary disks. This provides new possibilities for interpreting the light curves of such systems.

¹As usual in the analysis of observational data, the phase angle, ϕ , is measured from the line connecting the centers of the two stars, with the phase increasing in the direction opposite to the system’s rotation.

2 The Model

We used the model of [22] in our numerical study of the gas dynamics of the matter flows in a semidetached binary. We described the flow pattern using a three-dimensional system of gravitational gasdynamical equations including the effects of radiative heating and cooling of the gas:

$$\left\{ \begin{array}{l} \frac{\partial \rho}{\partial t} + \text{div } \rho \mathbf{v} = 0, \\ \frac{\partial \rho \mathbf{v}}{\partial t} + \text{div}(\rho \mathbf{v} \otimes \mathbf{v}) + \text{grad } P = -\rho \text{grad } \Phi - 2[\boldsymbol{\Omega} \times \mathbf{v}]\rho, \\ \frac{\partial \rho(\varepsilon + |\mathbf{v}|^2/2)}{\partial t} + \text{div } \rho \mathbf{v}(\varepsilon + P/\rho + |\mathbf{v}|^2/2) = \\ -\rho \mathbf{v} \text{grad } \Phi + \rho^2 m_p^{-2} (\Gamma(T, T_{wd}) - \Lambda(T)). \end{array} \right. \quad (1)$$

Here ρ is the density, $\mathbf{v} = (u, v, w)$ the velocity vector, P the pressure, ε the internal energy, Φ the Roche potential, m_p the proton mass, and $\Gamma(T, T_{wd})$ and $\Lambda(T)$ the radiative heating and cooling functions, respectively. The system of gas-dynamical equations was closed with the equation of state for an ideal gas, $P = (\gamma - 1)\rho\varepsilon$, where γ is the adiabatic index. The parameter was taken to be $5/3$.

We solved this system of equations using the Roe–Osher technique [21, 25, 26] adapted for multiprocessor computers. The modeling was carried out in a noninertial frame of reference rotating with the binary, in Cartesian coordinates, on a rectangular three-dimensional grid. Since the problem is symmetric about the equatorial plane, we modeled only half of the space occupied by the disk. The size of the modeled region, $1.12A \times 1.14A \times 0.17A$ (where A is the distance between the system's components), was chosen to completely include the disk and the stream of matter from the point L_1 . The computational grid had $121 \times 121 \times 62$ cells distributed among 81 processors forming a 9×9 two-dimensional array. The grid was made denser in the region of interaction between the stream and the disk in order to improve the accuracy of the solution in this region. The grid was also denser near the equatorial plane, providing good resolution of the disk's vertical structure.

The solution obtained for the model without cooling was used for the initial conditions [27]. Before the solution converged, the model with cooling was computed for ≈ 5 orbital periods of the system as a whole. The total computation time was ≈ 1000 hours at the MVS 1000A computer of the Joint Supercomputer Center (JSCC).

A free boundary condition with constant density $\rho_b = 10^{-8}\rho_{L_1}$, a temperature of 13600° K , and zero velocity was imposed at the outer boundaries of the computational domain (except near L_1), where L_1 is the matter density at L_1 . The accretor was taken to be a sphere of radius $10^{-2}A$. All the matter entering the accretor cells was taken to fall onto the star. The stream was specified as a boundary condition: matter with temperature 5800° K , density $\rho_{L_1} = 1.6 \times 10^{-8} \text{ g/cm}^3$, and velocity along the x axis $v_x = 6.3 \text{ km/s}$ was injected into a region with radius $0.014A$ around L_1 .

We considered a semi-detached binary consisting of a donor with mass M_2 that fills its Roche lobe and an accretor with mass M_1 . The following parameters were adopted for the system: $M_1 = 1.02M_\odot$, $M_2 = 0.5M_\odot$, and $A = 1.42R_\odot$, corresponding to $P_{orb} = 3.79^h$. The disk in the model had a temperature of 13600° K . For the specified rate of matter entering the system, the corresponding accretion rate in the model was $\approx 10^{-10}M_\odot/\text{yr}$.

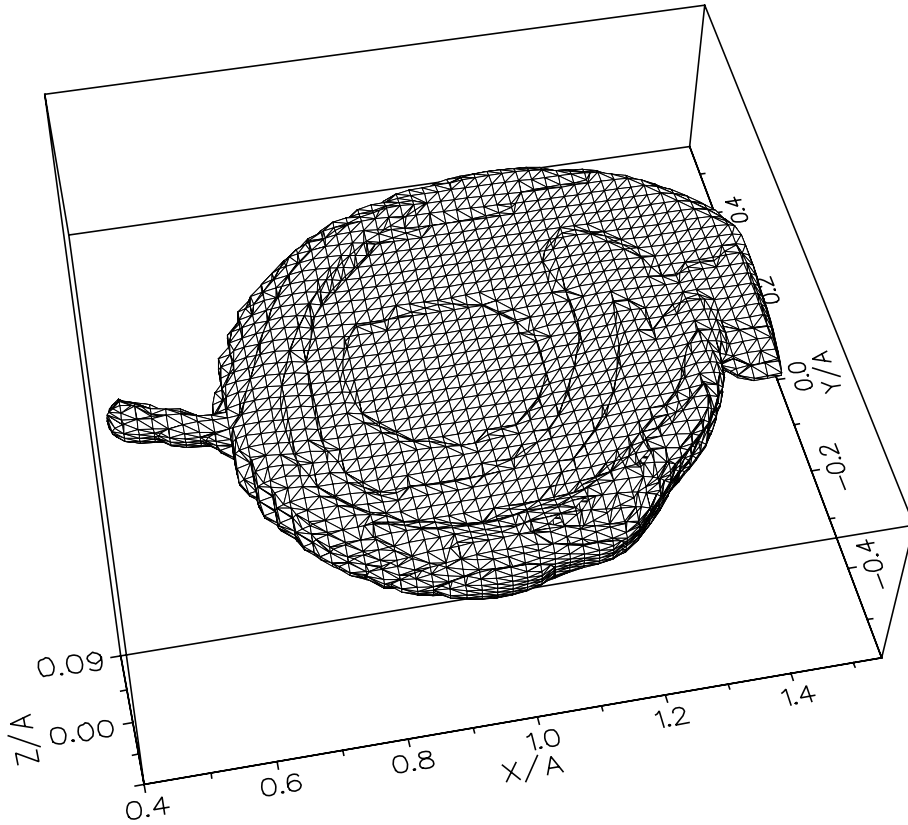


Figure 2: Three-dimensional surface of constant density $\rho = 5 \times 10^{-11} g/cm^3$.

3 Results of the Computations

We described the morphology of the matter flows in a semi-detached binary with a stationary, cool ($T = 13600^\circ K$) disk in [22]. Let us briefly summarize the main features of the computed flow structure. Figure 2 shows the three-dimensional surface of constant density $\rho = 5 \times 10^{-11} g/cm^3$. The region of the interaction between the stream and circumdisk halo is shown enlarged in Fig. 3 [22, Figs. 7, 8]. The left panel of Fig. 3 displays contours of constant density and velocity vectors, while the right panel of Fig. 3 is the so-called texture: a visualization of the velocity field by means of numerous tracks of test particles.

The results presented demonstrate that the interaction between the circumdisk halo and the stream possesses all the characteristic features of an oblique collision of two flows. The resulting structure of two shock waves with a tangential discontinuity between them is clearly visible in Fig. 3. The region of the shock interaction between the stream and halo has a complex shape. The parts of the halo far from the disk have low density, and the shock due to their interaction with the stream lies along the edge of the stream. The shock bends as the gas density in the halo increases, finally assuming a position along the edge of the disk. Note that the solution for the cool case has the same qualitative features as the solution for hot outer parts of the disk [27]: the interaction between the stream and the disk is collisionless, the region of enhanced energy release is due to the interaction between the gas in the circumdisk halo and in the stream and is located outside the disk, and the resulting system of shocks is extended and can be considered as a "hot line".

It follows from the above general features of the flow pattern that, at the interaction zone, the halo gas and stream gas pass through the shocks corresponding to their own flows, are

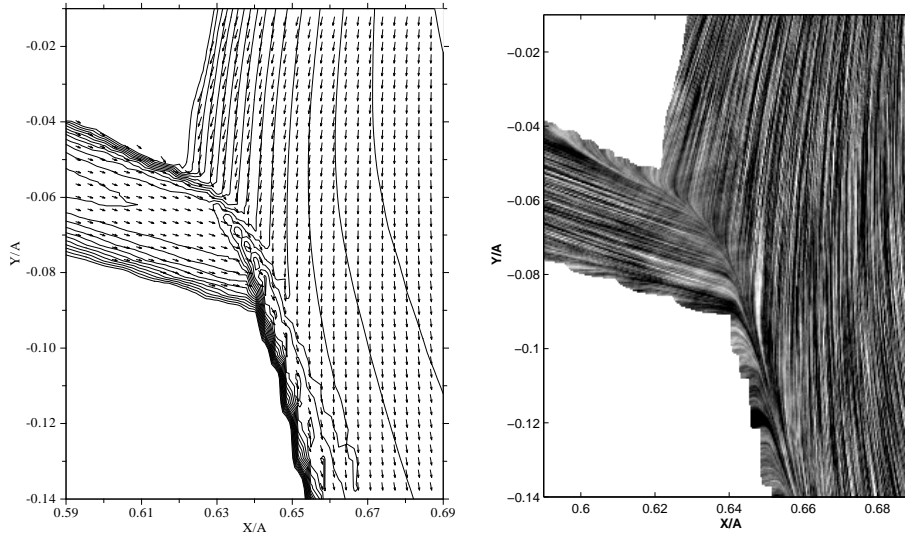


Figure 3: Contours of constant density and velocity vectors (left panel) and a visualization of the velocity field (right panel) in the region of interaction between the stream and the circumdisk halo, in the system's equatorial plane. This figure was first published in [22].

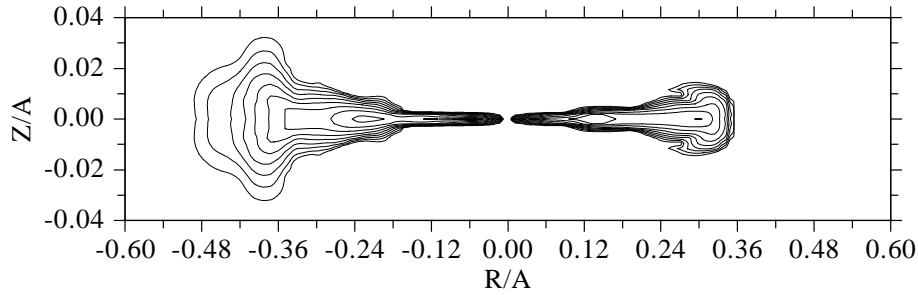


Figure 4: Contours of constant density in the section of the flow structure perpendicular to the equatorial plane and passing through the accretor and the region of the halo's maximum thickening ($\phi = 0.7$).

mixed, and then move along the tangential discontinuity between the two shocks. Subsequently, the disk itself, halo, and inter-component envelope are formed of precisely this matter. The jump in the gas parameters after the passage of the shock leads to a the increase of density and temperature in the region between the shocks and, consequently, to the appearance of a pressure gradient along the z axis, perpendicular to the system's plane of rotation. As a result, the gas begins to expand vertically, increasing the z component of the velocity, until the pressure gradient is balanced by the gravitational force.

The vertical gas pressure due to the presence of the z component of the velocity, together with the motion of the gas along the tangential discontinuity at the disk's outer edge, lead to a gradual increase of the thickening of the circumdisk halo (along the z axis). This thickening of the halo along the outer edge of the accretion disk is clearly visible in the three-dimensional constant-density surface shown in Fig. 2, as well as in Fig. 4, which displays constant density curves in the section of the flow structure that is perpendicular to the equatorial plane and drawn through the accretor and the maximum thickening of the halo ($\phi = 0.7$). An additional illustration of the halo thickening above the disk is provided by Fig. 5, which shows fragments

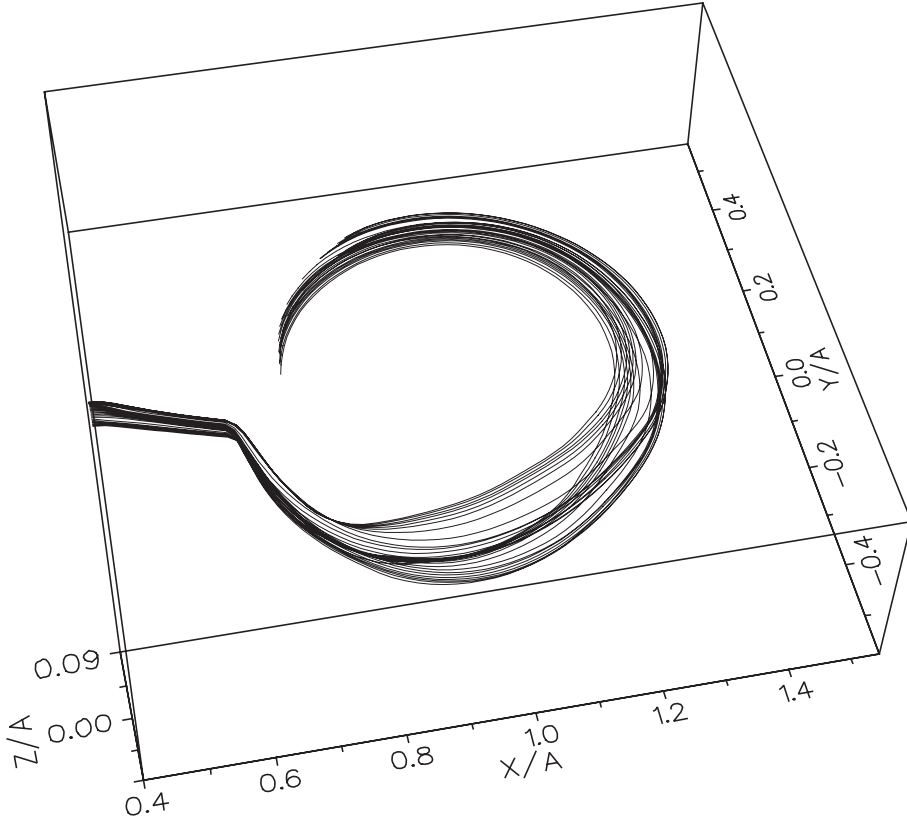


Figure 5: Fragments of streamlines emerging from the neighborhood of L_1 .

of computed streamlines emerging from the vicinity of L_1 . We can see that the streamlines diverge after acquiring a vertical acceleration in the region between the shocks, then converge again toward the system's equatorial plane. The region of vertical acceleration is restricted to the hot-line zone. After passing this region, the gas has a large vertical velocity component that makes it climb higher, until its store of kinetic energy is exhausted. The point where the upward motion ceases corresponds to the maximum height, which is reached at phase ~ 0.7 , i.e., already substantially outside the hot line.

To quantitatively analyze the thickening of the halo above the disk, let us consider the behavior of the streamlines and the distributions of the gas parameters along them. In a cylindrical coordinate system with its origin coincident with the accretor ($x = A, y = 0.0, z = 0.0$) and the angle ϕ measured from the point L_1 opposite to the direction of rotation of the matter (coincident with the system's direction of rotation), each point of the streamline is described by the coordinates (r, ϕ, z) . The $z(\phi)$ relations for four streamlines originating at points in the neighborhood of L_1 are presented in Fig. 6. We can see that, after entering the hot-line region (phase ~ 0.975), the streamlines begin to climb due to the increase of the velocity's z component. The phase relation of the vertical velocity for the same four streamlines is displayed in Fig. 7. When the gas emerges from the hot line (phase ~ 0.8), the force due to the pressure jump behind the shocks disappears, and the gas simply moves in the accretor's gravitational field. The vertical velocity of the gas becomes zero at phase ~ 0.7 , corresponding to the maximum ascent of the streamlines. The height of the halo at this position reaches $\sim 0.04A$.

In addition to the primary maximum, the system also exhibits a minimum height at phase

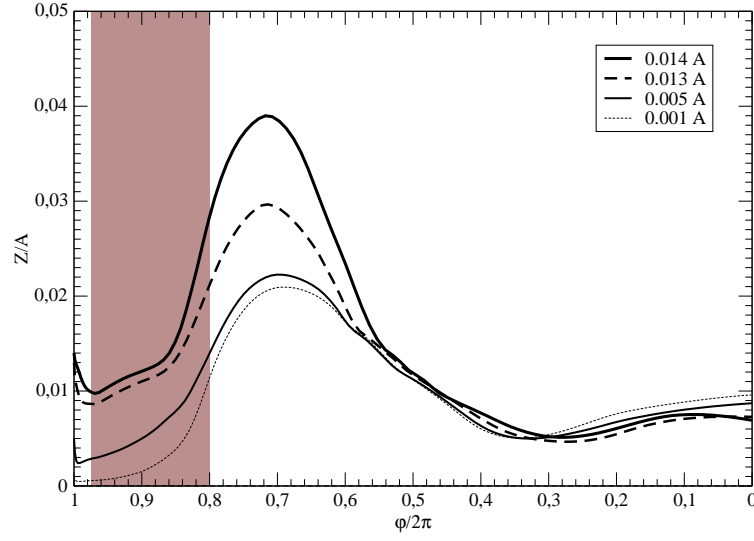


Figure 6: $z(\phi)$ relation for four streamlines. The streamlines originate in the vicinity of L_1 and have the coordinates $(x_{L_1}, 0, z_0)$. The z_0 values for each streamline are indicated in the plot. The shaded area corresponds to the region where v_z increases.

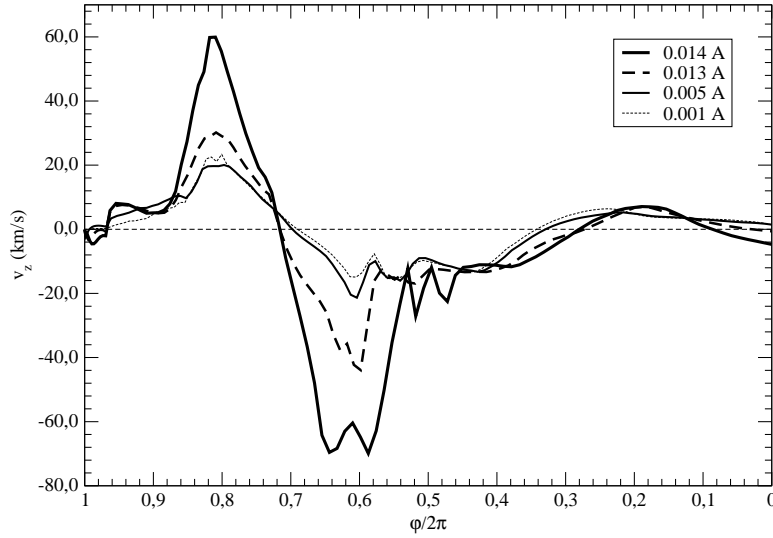


Figure 7: $V_z(\phi)$ relation along the same four streamlines as in Fig. 6.

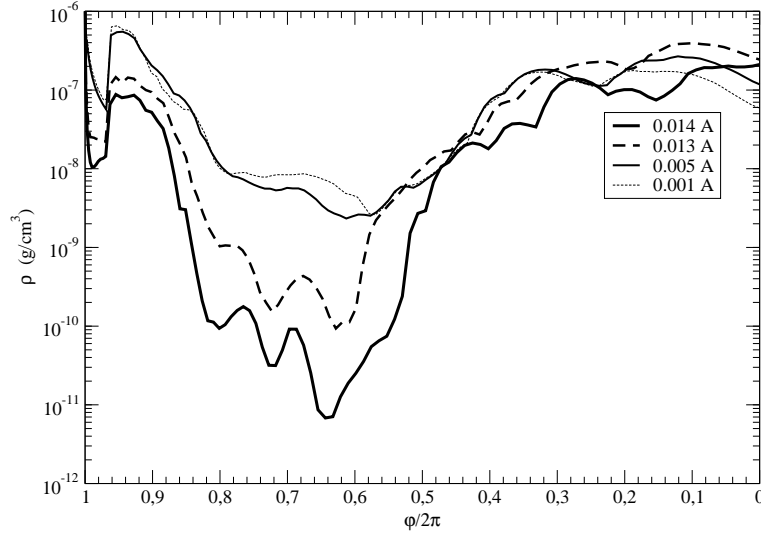


Figure 8: The density relation $\rho(\phi)$ along the same four streamlines as in Fig. 6.

~ 0.3 , when $z \sim (0.005 \div 0.006)A$, and a secondary maximum at phase ~ 0.1 , when the height of the halo is $\sim 0.01A$. Due to the effects of viscous dissipation, the minimum and secondary maximum are considerably less pronounced than the primary maximum. Eventually, viscosity leads to complete damping of the vertical velocity oscillations, so that the gas no longer possesses a significant vertical velocity when it next approaches the region of the interaction with the stream.

Figure 8 is the phase dependence of the density for the same four streamlines as in Fig. 6. The densities correspond to the mass-exchange rate in the RW Tri system ($10^{-8} M_{\odot}/yr$ [28]). We can see from these results that a strong density decrease is observed in the region of maximum ascent of the streamlines. This behavior of the density can lead to a displacement of the light-curve dips towards regions of higher ρ ; i.e., towards higher phases. This should be manifest most strongly in short-wavelength observations, since higher densities are required to absorb harder radiation. It is also interesting that the gas density is much higher near the secondary maximum, at phases ~ 0.1 , than near the first thickening.

To evaluate whether the central source can be eclipsed by the thickening of the halo, we computed the optical depth of the halo matter, τ . The optical depth is the product of the density, the layer's geometrical depth, and the absorption coefficient: $\tau = \rho l \kappa$. To estimate τ near the region of thickening, let us use the densities presented in Fig. 8, taking the characteristic linear size of the thickening to be its halfheight (Fig. 6). We estimate the absorption coefficient using the approximation formulas from [29] with a temperature of $\sim 13600^{\circ}K$ and a characteristic density corresponding to the value at the thickening's half maximum. Our estimates of τ are presented in Fig. 9, which shows the relations between the optical depth and the phase, $\tau(\phi)$, along the same four streamlines as in Fig. 6. An analysis of these estimates of τ shows that the thickening is optically thick, even at its greatest heights, and the value of τ at the half maximum can reach $\sim 10^2$. This means that the halo thickening is capable of eclipsing the central source, giving rise to the dips observed in the light curves of semi-detached binaries with stationary disks.

Obviously, in stationary systems, when there is no collision between the stream and the outer edge of the disk, there can be no ricochet and no transfer of a substantial fraction of the stream's matter into the inner parts of the disk. However, the momentum of the stream matter

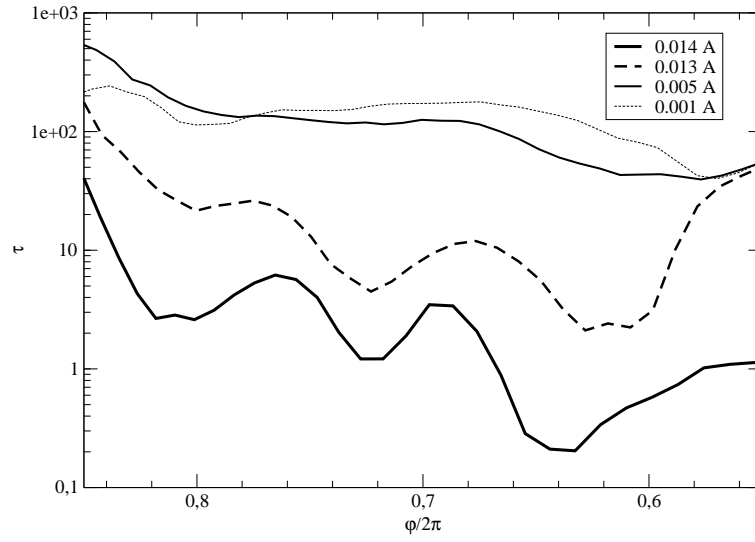


Figure 9: The optical depth relation, $\tau(\phi)$, near the thickening ($\phi = 0.55 \div 0.85$) along the same four streamlines as in Fig. 6.

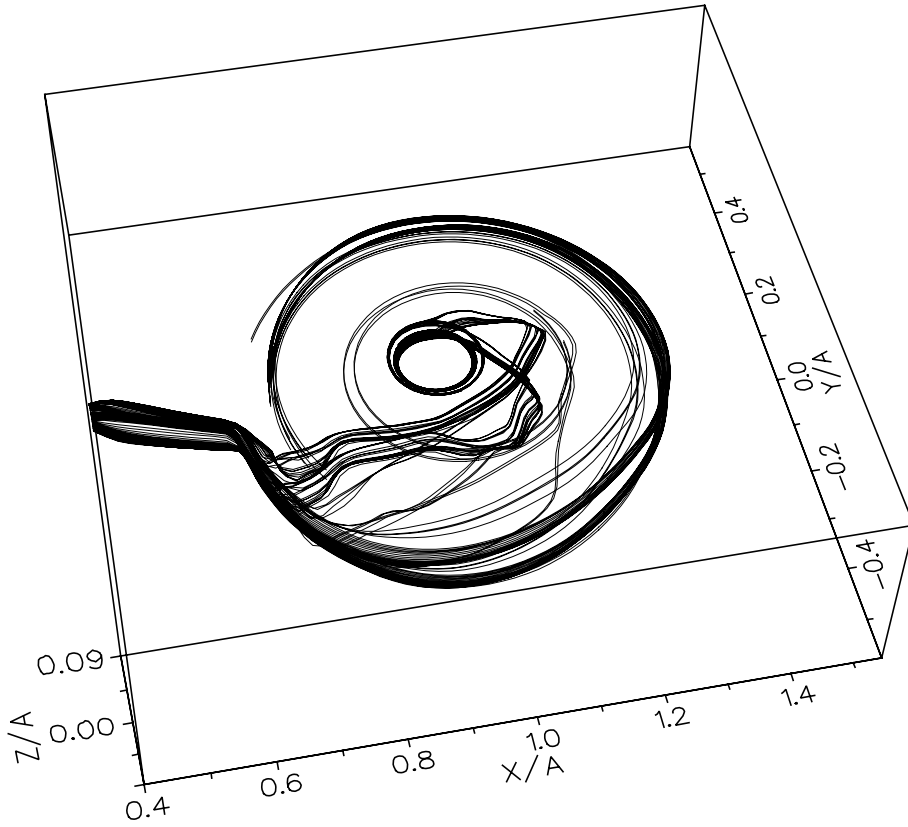


Figure 10: Same as Fig. 5, also showing fragments of the streamlines emerging from a wider vicinity of L_1 .

is lower than that of the halo gas, so that some of the stream gas at great heights can slide down into inner orbits, appearing as if the stream is flowing around the outer edge of the disk. This sliding-down can take place only in the hot-line region, where the momenta of the matter in the stream and in the halo have not yet become equalized. Indeed, when considering the streamlines that reach high heights from the stream's center (Fig.10), we can see that some of them leave the interaction region of the stream and halo, envelop the disk from the upper side, and get into its inner regions. The results of our computations demonstrate that the total flux of matter associated with this effect is small, and apparently cannot significantly influence the visibility of the central object.

4 Conclusions

Observations of semi-detached binaries with stationary accretion disks reveal dips in their light curves at phase ~ 0.7 . These dips are usually explained by invoking the presence of a thickening at the outer edge of the accretion disk, without explaining how matter appears at considerable heights above the accretion disk in the case of a stationary interaction between the stream and disk. It is important to resolve the problem of the formation of this thickening of the halo above a stationary disk if we wish to correctly interpret the observations and more fully understand the nature of matter-exchange processes in these stars.

The results of our three-dimensional numerical modeling of the matter-flow structure in semidetached binaries with stationary disks confirm our earlier conclusions [21, 22, 27] that the interaction between the stream and disk is collisionless, the region of increased energy release is due to the interaction between the gas in the circumdisk halo and the stream and is located outside the disk, and the system of shocks that forms is extended and can be considered as a "hot line." The interaction between the circumdisk halo and the stream possesses all the characteristic features of an oblique collision of two flows that results in the formation of a structure consisting of two shock waves and a tangential discontinuity.

In the hot-line region, the halo and stream gases pass through the shocks corresponding to their own flows, are mixed, and then move along the tangential discontinuity between the two shocks. During the interaction between the stream and the circumdisk halo, a considerable fraction of the matter acquires a vertical acceleration. The vertical motion of the gas due to the z component of the velocity, together with its motion along the tangential discontinuity at the outer edge of the disk, results in a gradual growth of the thickness of the circumdisk halo. The region of vertical acceleration is restricted to the hot-line zone, and its angular size does not exceed $\sim 65^\circ$. However, once it has passed this region, the gas has a sufficiently large vertical velocity component to rise until its store of kinetic energy is exhausted. The point where the upward motion ceases corresponds to the maximum height, which is reached at phase ~ 0.7 , already substantially outside the hot line. The thickening extends appreciably higher than the scale height of the disk, reaching values $\sim 0.04A$ (this corresponds to a ratio of the thickening's height to the distance to the accretor > 0.1), and its angular size exceeds $\sim 130^\circ$. Our computations also show that, in addition to the primary maximum, the system also displays a height minimum at phase ~ 0.3 , when $z \sim (0.005 \div 0.006)A$, and a secondary maximum at phase ~ 0.1 , when the height of the halo is $\sim 0.01A$.

Our analysis of these results leads us to conclude that the dips in the light curves of semi-detached binaries with stationary disks (i.e., in the absence of a collisional interaction between the stream and disk), can be explained by the formation of a thickening of the halo above the outer edge of the disk. The origin of this thickening is described well by the hot-line model, and

its quantitative features are consistent with observations. The proposed model can be applied to both semi-detached systems (LMXBs, cataclysmic variables) in their stationary state and to dwarf novae in outburst, provided that the outer parts of the disk are not strongly distorted in the outburst.

5 Acknowledgments

This study was supported by the Russian Foundation for Basic Research (project nos. 03-0216622, 03-01-00311, 05-02-16123, 05-02-17070, and 05-02-17874), the Program of Support for Leading Scientific Schools of Russia (grant no. NSh162.2003.2), and the basic-research programs "Mathematical Modeling and Intellectual Systems" and "Unstable Phenomena in Astronomy" of the Presidium of the Russian Academy of Sciences.

6 References

1. N. E. White and S. S. Holt, *Astrophys. J.* 257, 318 (1982).
2. K. O. Mason, in *Two Topics in X-ray Astronomy*, Vol. 1: X-ray Binaries, ESA SP-296, p. 113 (1989).
3. M. Livio, N. Soker, and R. Dgani, *Astrophys. J.* 305, 267 (1986).
4. R. Dgani, M. Livio, and N. Soker, *Astrophys. J.* 336, 350 (1989).
5. M. Hirose, Y. Osaki, and S. Mineshige, *Publ. Astron. Soc. Jpn.* 43, 809 (1991).
6. S. H. Lubow and F. H. Shu, *Astrophys. J.* 198, 383 (1975).
7. S. H. Lubow and F. H. Shu, *Astrophys. J.* 207, L53 (1976).
8. S. H. Lubow, *Astrophys. J.* 340, 1064 (1989).
9. J. Frank, A. R. King, and J.-P. Lasota, *Astron. Astrophys.* 178, 137 (1987).
10. P. J. Armitage and M. Livio, *Astrophys. J.* 470, 1024 (1996).
11. K. O. Mason, F. A. Cordova, M. G. Watson, and A. R. King, *Mon. Not. R. Astron. Soc.* 232, 779 (1988).
12. K. S. Long, C. W. Mauche, J. C. Raymond, et al., *Astrophys. J.* 469, 841 (1996).
13. T. Naylor, G. T. Bath, P. A. Charles, et al., *Mon. Not. R. Astron. Soc.* 231, 237 (1988).
14. I. Billington, T. R. Marsh, K. Horne, et al., *Mon. Not. R. Astron. Soc.* 279, 1274 (1996).
15. E. T. Harlaftis, B. J. M. Hassall, T. Naylor, et al., *Mon. Not. R. Astron. Soc.* 257, 607 (1992).
16. K. O. Mason, J. E. Drew, and C. Knigge, *Mon. Not. R. Astron. Soc.* 290, L23 (1997).
17. C. S. Froning, K. S. Long, and C. Knigge, *Astrophys. J.* 584, 433 (2003).
18. D. V. Bisikalo, A. A. Boyarchuk, O. A. Kuznetsov, and V. M. Chechetkin, *Astron. Zh.* 74, 880 (1997) [*Astron. Rep.* 41, 786 (1997)].
19. D. V. Bisikalo, A. A. Boyarchuk, O. A. Kuznetsov, et al., *Astron. Zh.* 75, 40 (1998) [*Astron. Rep.* 42, 33 (1998)].
20. D. V. Bisikalo, A. A. Boyarchuk, V. M. Chechetkin, et al., *Mon. Not. R. Astron. Soc.* 300, 39 (1998).
21. A. A. Boyarchuk, D. V. Bisikalo, O. A. Kuznetsov, and V. M. Chechetkin, *Mass Transfer in Close Binary Stars* (Taylor and Frances, London, 2002).
22. D. V. Bisikalo, A. A. Boyarchuk, P. V. Kaigorodov, and O. A. Kuznetsov, *Astron. Zh.* 80, 879 (2003) [*Astron. Rep.* 47, 809 (2003)].

23. M. Makita, K. Miyawaki, and T. Matsuda, *Mon. Not. R. Astron. Soc.* 316, 906 (2000).
24. K. Sawada and T. Matsuda, *Mon. Not. R. Astron. Soc.* 255, 17P (1992).
25. P. L. Roe, *Ann. Rev. Fluid Mech.* 18, 337 (1986).
26. S. R. Chakravarthy and S. Osher, in *Proceedings of the 23rd Aerospace Sci. Meeting*, AIAA-85-0363, p. 363 (1985).
27. O. A. Kuznetsov, D. V. Bisikalo, A. A. Boyarchuk et al, *Astron. Zh.* 78, 997 (2001) [*Astron. Rep.* 45, 872 (2001)].
28. P. J. Groot, R. G. M. Rutten, and J. van Paradijs, *Astron. Astrophys.* 417, 283 (2004).
29. K. R. Bell and D. N. C. Lin, *Astrophys. J.* 427, 987 (1994).